

## Stabilization of insulin using low molecular weight chitosan carbonate nanocarrier

Mayyas Al-Remawi<sup>a,\*</sup>, Nisrein Jaber<sup>b</sup>, Amani Elsayed<sup>c</sup>, Diya Alsafadi<sup>d</sup>, Khalid Abu Salah<sup>e</sup>

<sup>a</sup> Faculty of Pharmacy and Medical Sciences, University of Petra, Amman 11196, Jordan

<sup>b</sup> Faculty of Pharmacy, Al-Zaytoonah University of Jordan, Amman 11733, Jordan

<sup>c</sup> Faculty of Pharmacy, Taif University, Taif 21974, Saudi Arabia

<sup>d</sup> Scientific Research Center, Royal Scientific Society, Amman 11941, Jordan

<sup>e</sup> King Abdullah International Medical Research Center, King Saud bin Abdulaziz University for Health Sciences, Ministry of National Guard, Riyadh, Saudi Arabia

### ARTICLE INFO

#### Keywords:

Insulin  
Chitosan  
Carbonate divalent anions  
Stability  
Nanocarrier

### ABSTRACT

The current study aims to design a nanoparticulate system that could encapsulate insulin and improve its stability. Nanoparticles were formulated by ionic cross-linking of chitosan (CS) with carbonate divalent anions. The interaction between the two moieties was evidenced by AFM, FTIR and surface tension measurements. CS carbonate nanoparticles were prepared with different mole fractions. The mole fraction of carbonate that produced the smallest size nanoparticles and highest zeta potential (40 nm and +39 mV, respectively) was determined. Circular dichroism (CD) studies revealed that insulin conformation was not affected by CS at 20 °C. However, the studies at elevated temperatures demonstrated that CS had a role in insulin stabilization. Fluorescence spectroscopy indicated the interaction between insulin and CS carbonate. The findings from this investigation showed the potential use of CS carbonate as an insulin stabilizer and at the same time as an insulin nanocarrier system.

### 1. Introduction

Diabetes mellitus is an endocrine disorder results in elevating blood glucose level (Jarrar, Al-Essa, Kilani, Hasan, & Al-Qerem, 2018). Exogenous insulin is usually administered by subcutaneous injection to treat diabetic type I patients (Rull et al., 2005). However, insulin is a delicate protein molecule. Its three-dimensional structure could be easily disrupted during formulation, manufacturing and storage. Excipients are added to preserve the stability of this challenging molecule. Polysorbates (non-ionic surfactants) are classical insulin stabilizers which are used in commercial products to minimize adsorption and aggregation. Recently, many concerns about their usage in protein formulations have been raised. Polysorbates contain polyoxyethylene moiety that undergoes autoxidation and form peroxides that damage protein's structure and increase its immunogenicity (Maggio, 2012). These problems make the search for alternative stabilizers a necessity.

Rasmussen, Tantipolphan, van de Weert, and Jiskoot (2010) examined the effect of molecular chaperone  $\alpha$ -crystallin on insulin's physical stability and compared it with common stabilizers. The molecular chaperone  $\alpha$ -crystallin demonstrated superior stabilizing effect

compared to human serum albumin, polysorbate 80 and sucrose. Other studied insulin's stabilizers were modified sugars, zwitterionic and trehalose degradable polymers and natural polymers such as gelatin and chitosan (CS) (Piccinini et al., 2022, Pelegri-O'Day et al., 2020, Jayamani & Shanmugam, 2016, Elsayed, Al Remawi, Qinna, Farouk, & Badwan, 2009). Actually, CS is considered an interesting polymer which was used as a carrier for delivery of both chemical and protein-based ingredients that control diabetes mellitus such as metformin (Lari, Zahedi, Ghourchian, & Khatibi, 2021), glipizide (Kar & Pati, 2019), extindin-4 (Lee et al., 2013) and insulin (Sharma, Arora, Banerjee, & Singh, 2021).

Nano delivery systems were also explored to suppress aggregation of biopharmaceuticals. Nanoparticles showed high potential in protecting insulin from thermal and chemical aggregation (Das, Chakrabarti, & Das, 2015). However, the effect of nanoparticles on protein's stability depends on surface chemistry of the nanoparticles and intrinsic protein stability (Cabaleiro-Lago and Lins, 2012). Herein, we investigated the stability of insulin incorporated in CS-carbonate nanocarrier.

CS has gained considerable attention due to its biocompatibility, biodegradability, non-immunogenicity, non-toxicity, and ability to

\* Corresponding author.

E-mail addresses: [malremawi@uop.edu.jo](mailto:malremawi@uop.edu.jo) (M. Al-Remawi), [n.jaber@zu.edu.jo](mailto:n.jaber@zu.edu.jo) (N. Jaber), [e.amani@tu.edu.sa](mailto:e.amani@tu.edu.sa) (A. Elsayed), [diya.safadi@rss.jo](mailto:diya.safadi@rss.jo) (D. Alsafadi), [abu-salah@ngha.med.sa](mailto:abu-salah@ngha.med.sa) (K.A. Salah).

<https://doi.org/10.1016/j.carbpol.2022.119579>

Received 16 February 2022; Received in revised form 9 April 2022; Accepted 4 May 2022

Available online 11 May 2022

0144-8617/© 2022 Elsevier Ltd. All rights reserved.

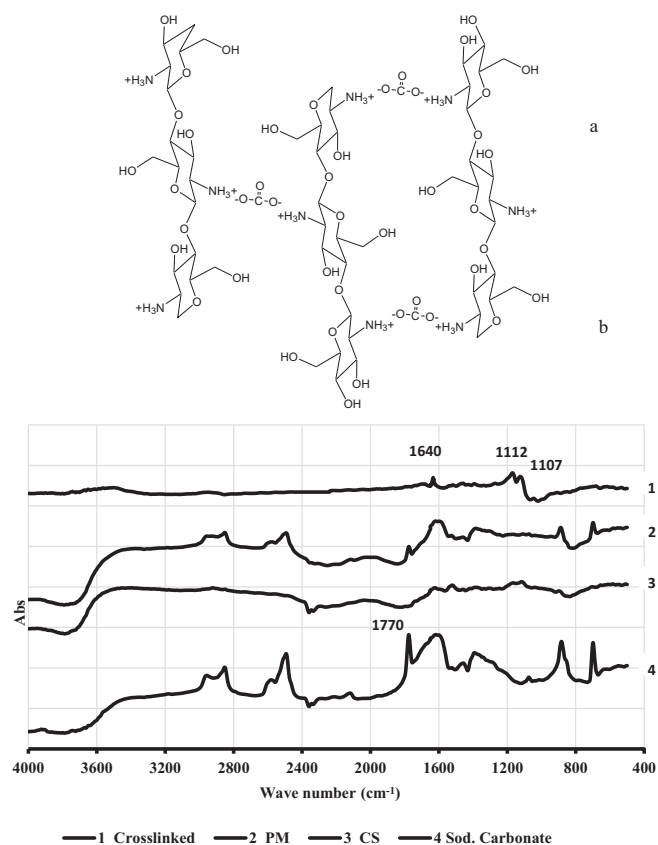
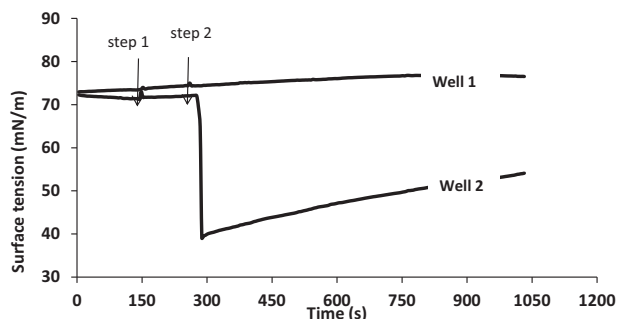


**Fig. 1.** CS carbonate structural changes upon crosslinking (a) schematic representation of CS polymer upon crosslinking with carbonate divalent anions. (b) FTIR of 1—crosslinked CS carbonate, 2—physical mixture (PM) of CS/sodium carbonate, 3—CS and 4—sodium carbonate.



Time(s)	Well-1 (control)	Well-2
0	1ml water	1ml water
150	add 0.1 ml water	add 0.1 ml CS (10mg/10ml water)
250	add 0.1 ml water	add 0.1 ml Na <sub>2</sub> CO <sub>3</sub> (1g/100ml)

**Fig. 2.** Surface tension kinetics after the sequential addition of CS and sodium carbonate (Well 2) and water additions (Well 1) (control). The attached Table describes the sequence of addition.

enhance the absorption of peptides and proteins (Chen et al., 2013; Ma & Lim, 2003). Nano-polymeric colloids formulated from CS have been explored as carrier systems for in vivo delivery of insulin and showed promising results (Al-Remawi, Elsayed, Maghrabi, Hamaidi, & Jaber, 2017; Badwan et al., 2009; Elsayed et al., 2009; Elsayed et al., 2011). Different methods for fabrication of CS nanoparticles were discussed in literature (Du, Luo, Xu, & Chen, 2007; Grenha, 2012). However, ionotropic gelation of CS with polyanions remains the most popular method

for delivery of peptides and proteins. The delicate structures of these molecules were preserved during processing as this method does not involve high temperature or organic solvents. Polyanions such as triphosphate, sulfate, citrate, poly [ $\gamma$ -glutamic acid], were proposed as crosslinking agents for CS (Al-Remawi, 2012; Bagheri, Younesi, Hajati, & Borghei, 2015; Diop et al., 2015; Lin et al., 2005). Recently, carbonate anions were used to crosslink high molecular weight CS excipient. The excipient was used to produce orally dispersible solid pharmaceutical formulations (Al-Remawi & Al-Akayleh, 2020). The aim of this study is to investigate stability of insulin loaded in low molecular weight (LMW) CS carbonate nanoparticles produced by ionotropic gelation as a formulation prerequisite for development of buccal insulin delivery system. The study demonstrates the importance of using CS polysaccharide as delivery system in disease treatment through simple chemical modifications leading to low-cost natural medicine. Factors affecting the delivery system were characterized by FTIR, surface tension, particle size, zeta potential and atomic force microscope. The effect of changing pH and temperature on insulin physical stability was also evaluated. Moreover, circular dichroism (CD) and fluorescence microscopy studies were conducted to gain more information about conformation and secondary structures of free and encapsulated insulin.

## 2. Experimental

### 2.1. Materials

LMW CS was prepared by acid hydrolysis with a molecular weight average around 13 kDa and degree of deacetylation DDA of 100% according to our previous published work (Obaidat et al., 2010; Qandil et al., 2009). Rh-insulin was obtained from Sigma-Aldrich. Sodium carbonate, anhydrous was purchased from PRS Panreac Quimica SA, Spain.

### 2.2. Methods

#### 2.2.1. Preparation of CS/carbonate nanoparticles

The method was adopted with modifications according to Al-Remawi, 2012. 0.1% w/v LMW CS was prepared in 100 ml 0.01 M HCl with stirring at room temperature the pH of the solution was maintained in the acidic range i.e. 3.9–4. Another, 1% w/v sodium carbonate in 100 ml distilled water was prepared to produce the alkaline crosslinking solution. In another beaker, various volumes of carbonate solution were added drop wise to 10 ml 0.1% w/v CS solution while mixing using magnetic stirrer (900 rpm) for 2 min at ambient temperature to produce the nanoparticle dispersion at different molar ratios where, the changes in pH, particle size and zeta potential were monitored upon each addition.

#### 2.2.2. Preparation of CS/carbonate nanoparticles loaded with h-insulin

An amount of 44 mg insulin was dissolved in 10 ml 0.01 M HCl and the volume was completed with water up to 100 ml. To the previous insulin solution, 100 mg LMW CS was dissolved, then suitable amount of 1% w/v sodium carbonate solution was added drop wise with stirring using magnetic stirrer (900 rpm) for 2 min at ambient temperature, while monitoring the changes in pH, particle size and zeta potential.

#### 2.2.3. Surface tension kinetics

Surface tension kinetic study was conducted at room temperature using surface tensiometer (Kibron with KBN 315 sensor head, Finland). Two clean wells were used and the sequence of addition of solutions to the wells, each containing 1 ml double distilled water, was as follows:

Well-1: To 1 ml double distilled water, two portions of 0.1 ml double distilled water were added at 150 and 250 s sequentially (control).

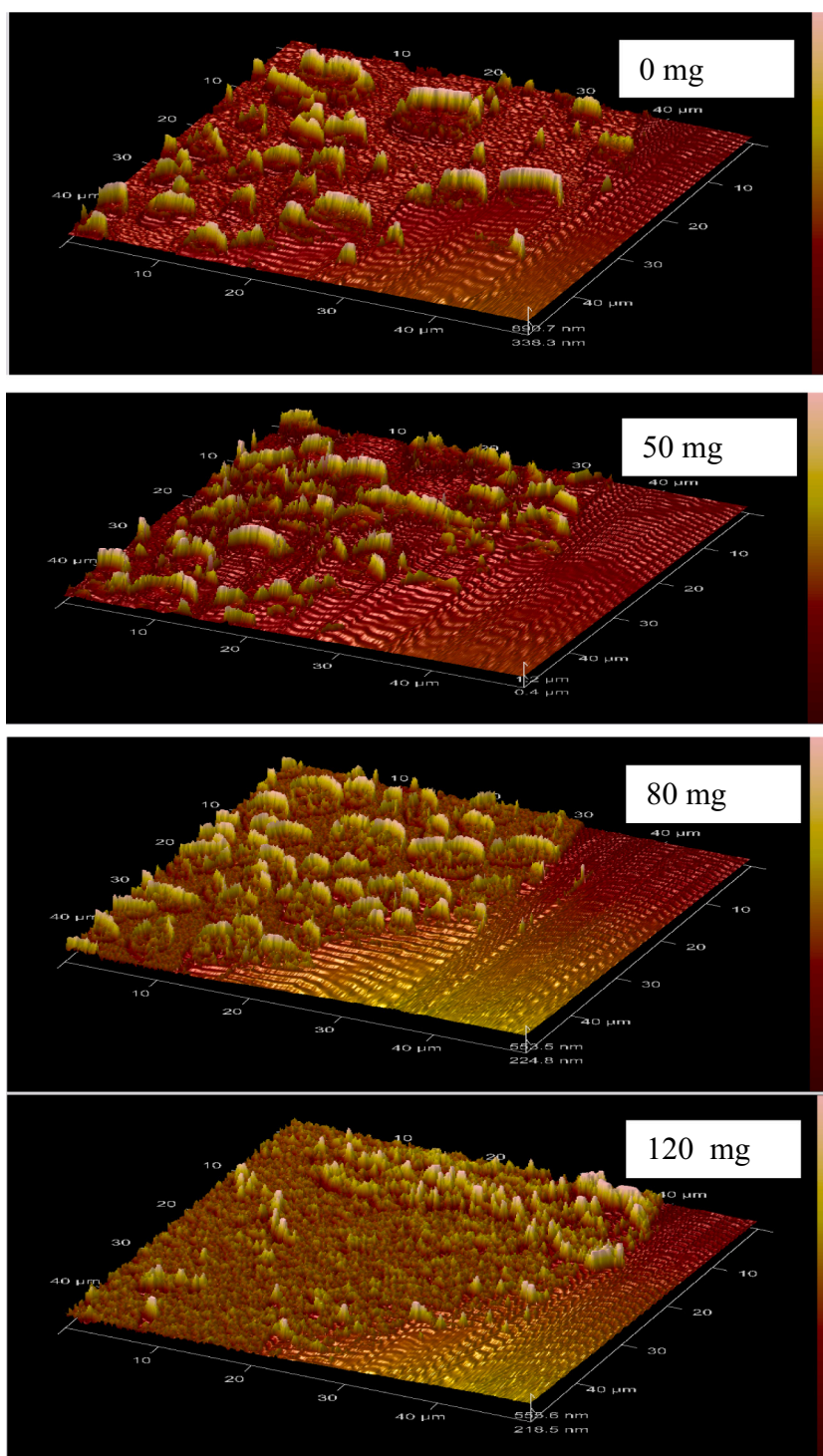


Fig. 3. AFM contact mode using MPP-AFM tips crosslinked CS carbonate upon the addition of sodium carbonate 0, 50, 80 and 120 mg to 10 ml 0.1% w/v CS. The scanned area  $50 \mu\text{m} \times 50 \mu\text{m}$ .

Well-2: To 1 ml double distilled water, 0.1 ml 0.1% w/v CS was added after 150 s then after 250 s another 0.1 ml of 1% w/v sodium carbonate was added.

#### 2.2.4. FTIR

The crosslinked CS carbonate was prepared as mentioned before and dried in an oven at  $40 \text{ }^\circ\text{C}$  for 48 h. The 10 mg powder samples of crosslinked CS carbonate, physical mixture of CS/sodium carbonate, CS and sodium carbonate were mixed individually with 200 mg KBr and a

disc was formed and Abs was measured using FTIR (Perkin-Elmer, UK).

#### 2.2.5. Atomic force microscopy (AFM)

Different amount of sodium carbonate (0, 50, 80 and 120 mg) were added to 10 ml of 0.1% w/v CS solutions to form crosslinked CS-carbonate nano-suspensions. The nano-suspensions were diluted with distilled water by 1:10 volume ratio. One drop sample was carefully spread as a very thin layer over a glass slide and the samples were left to dry in closed drying oven at  $35 \text{ }^\circ\text{C}$  for 4 h. The surface morphology of the

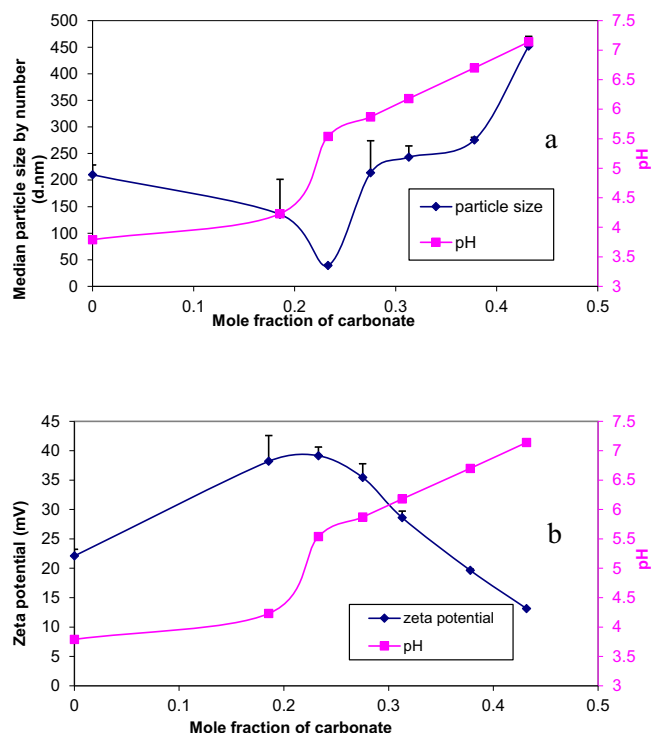


Fig. 4. Effect of mole fraction of carbonate reacted to glucosamine monomers present in CS on (a) changes in particle size and pH upon the addition of carbonate anion to CS solution and (b) changes in zeta potential and pH upon the addition of carbonate anion to CS solution.

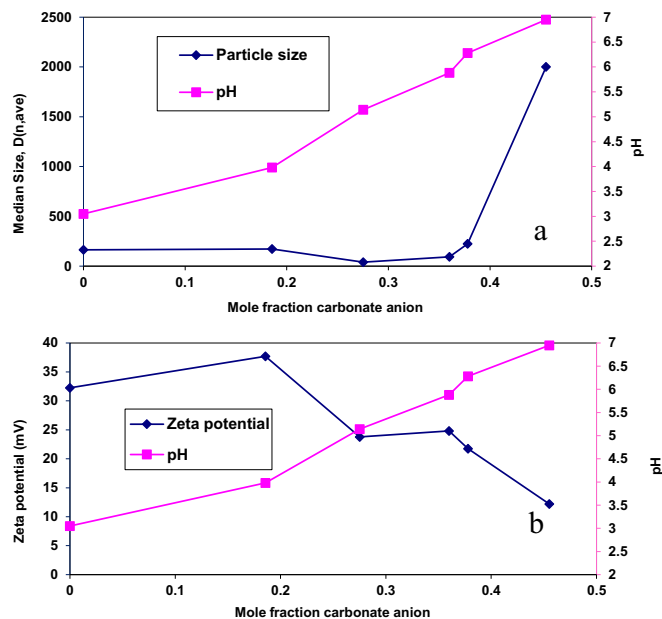


Fig. 5. Effect of mole fraction of carbonate anion to glucosamine monomers present in CS on (a) changes in particle size and pH upon the addition of carbonate anions to insulin/CS solution, and (b) changes in zeta potential and pH upon the addition of carbonate anion to insulin/CS solution.

produced smear particles was scanned using AFM (Dimension® Edge™ Atomic Force Microscope, Bruker). The AFM head is seamlessly integrated with light microscope instrumentation, were photos of the surface were taken prior to scanning by AFM. AFM photos were scanned using tapping mode operation with a tip model. AFM contact mode using

MPP-AFM tips composed of MPP-33220-W, 5 N/m, 40 kHz, Asymmetric Tip, Al Reflective.

#### 2.2.6. Particle size and zeta potential measurements

To a constant concentration of CS (1 mg/ml), different volumes of sodium carbonate were added drop wise with mixing to have a final concentration of sodium carbonate in the mixture in range of (0.15–0.55 mg/ml). Zeta potential and median particle size were determined for all samples using Zetasizer Nano ZS (Malvern Instruments, UK) at 25 °C. Five measurements with 10 runs were conducted and the average was calculated.

#### 2.2.7. pH changes

pH autotitration profiles of CS with carbonate anions were prepared as follows: sodium carbonate, alkaline solution, was used to titrate the positively charged CS. 1 g sodium carbonate was placed in 100 ml distilled water and used to titrate 25 ml of 0.1% w/v CS in 0.01 M HCl solution using the pH autotitrator unit attached to Zetasizer Nano-ZS (Malvern Instruments, UK) starting from pH around 3.5 until reaching 7.5. Similarly, the CS/insulin solution prepared as mentioned previously was also titrated with 1% w/v sodium carbonate solution.

#### 2.2.8. Loading capacity and encapsulation efficiency

To determine the effect of addition of carbonate anion on loading capacity and encapsulation efficiency of insulin, six samples were evaluated. Carbonate anion was added to CS in mole fractions of 0, 0.09, 0.22, 0.28, 0.36 and 0.4 to solutions containing constant concentration of insulin dissolved in 0.01 M HCl i.e. 0.4 mg/ml.

The amount of insulin loaded within nanoparticles has been described in our previous work (Elsayed et al., 2011). Briefly, to determine insulin loaded in CS carbonate nanoparticles, samples were centrifuged at 15,000 rpm for 30 min. Insulin content in the supernatant was assayed by high pressure liquid chromatography, HPLC (Thermo-spectra HPLC using TSP 1000 pump system with TSP 1000 UV-VIS detector and a TSP AS 3000 autosampler, Spectra System, USA). The conditions employed were as follows: the column was ACE 5  $\mu$ m, 250 mm  $\times$  5 mm i.d. and 300 Å pore size (ACE, Scotland); detection at 214 nm; eluent, acetonitrile-aqueous solution of 0.2 M sodium sulfate acidified with concentrated phosphoric acid to pH 2.3 (volume ratio 27:73); flow rate was 1 ml/min. The HPLC analytical method was verified in terms of linearity, specificity and precision (Elsayed et al., 2009). The inter and intra-day variability using different standard insulin concentrations were within a coefficient of variation CV below 2%.

Loading capacity (LC) was the percentage of actual mass of insulin loaded in nanoparticles to the total mass of nanoparticles, while the encapsulation efficiency (EE) was the percentage of the actual mass of insulin loaded in nanoparticles to the initial insulin mass used in the formulation of nanoparticles. The formulas for calculating LC and EE are as follows:

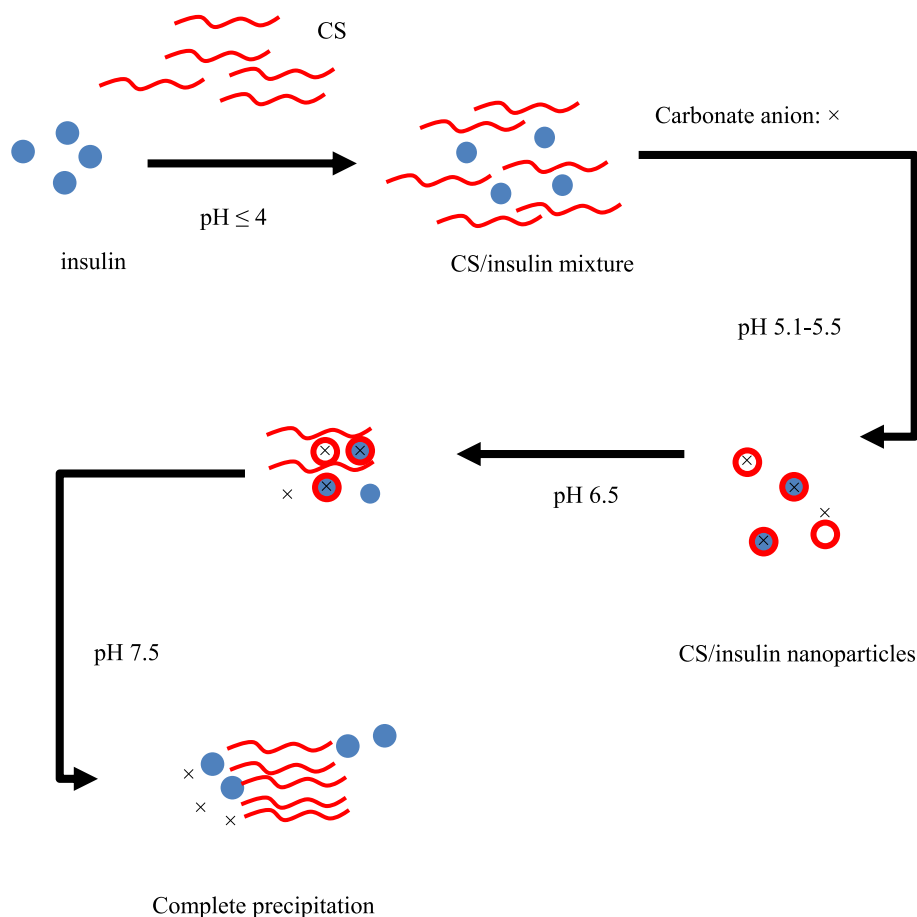
$$LC = \frac{M}{M_{NP}} \times 100 \quad (1)$$

$$EE = \frac{M}{M_{initial}} \quad (2)$$

in which M is the actual mass of insulin loaded in the nanoparticles,  $M_{NP}$  is the total mass of the nanoparticles, and  $M_{initial}$  is the initial mass of insulin used in the preparation of the nanoparticles (Raut, Doijad, Mohite, & Manjappa, 2018; Lu et al., 2019).

#### 2.2.9. Particle morphology

To determine the particle morphology of insulin loaded CS carbonate nanoparticles, scanning electron microscope, SEM (Phenom XL G2 scanning electron microscope, Thermo Fisher Scientific coupled with AXS EDS system) was used. The SEM images were collected at 6.10–4 Pa



**Scheme 1.** Demonstration of the formation of insulin loaded CS carbonate nanoparticles.

and with 15 kV accelerating voltage.

All samples were containing insulin at concentration of 0.4 mg/ml in 0.01 M HCl, then carbonate anions were added to CS at carbonate anion molar fractions 0, 0.28, 0.36 and 0.4. A single liquid drop specimen was placed onto the metal sample holder using an electrically conductive adhesive. The specimens were dried at room temperature in vacuum oven for 4–6 h until complete dryness. SEM images with magnifications 10,000 $\times$  were taken.

#### 2.2.10. *In vitro* release study

Insulin loaded CS carbonate samples were prepared as mentioned previously with insulin concentration (0.4 mg/ml) and carbonate anion mole fraction (0.36). The CS carbonate samples (10 ml) were placed in dialysis bags. The dialysis bags were put in 200 ml dissolution media. *In vitro* dissolution was carried out using USP Type-II paddle apparatus at rotational speed of 100 rpm and temperature  $37 \pm 0.5$  °C. The release media used was either 0.1 M HCl (pH 1.2) or USP phosphate buffer (pH 6.8) for 1 h. The release medium was withdrawn (1 ml) at regular time intervals and analyzed for insulin content using the HPLC method mentioned before.

#### 2.2.11. Particle size (Z-average) and thermal stability

Changes in particle size (Z-average) were used to evaluate the thermal stability of insulin loaded in CS carbonate (Elsayed, Al-Remawi, Maghrabi, Hamaidi, & Jaber, 2014). Z-average measurements were carried out with Zetasizer Nano ZS (Malvern Instruments, UK). Insulin-loaded in CS carbonate nanoparticles were diluted to final insulin concentration 0.1 mg/ml with pure dust free deionized water. Particle size measurements (Z-average) for free and encapsulated insulin were also performed in a temperature range 20–90 °C.

#### 2.2.12. Circular dichroism (CD)

CD spectra of free insulin and insulin loaded CS carbonate nanoparticles samples were determined at 20 °C with a total nitrogen flow of 5 l/min on Circular Dichroism Spectrometer (Chirascan, Applied Photophysics, England). All materials were prepared at insulin final concentration of 0.1 mg/ml and scanned from 190 to 280 nm, the time points were 0.5 and time interval was 0.1 ms. The effect of temperature on the spectra was also determined by heating the samples at constant rate (2 °C/min) starting from 25 to 80 °C with a scan range from 190 to 280 nm. Deconvolution was carried out using CDNN program (Dr. Gerald Böhm, Applied Photophysics, UK) and so the percentages of  $\alpha$ -helix,  $\beta$ -sheet and random coil in free and associated insulin were calculated accordingly (Elsayed et al., 2014).

#### 2.2.13. Fluorescence spectroscopy measurements

The fluorescence property of the Tyrosine [Tyr] residues was used to follow the interaction of insulin with CS carbonate nanoparticles. All of the fluorescence measurements were carried out using a Varian Cary Eclipse spectrofluorimeter. Insulin loaded CS carbonate nanoparticle sample was incubated for 24 h. To estimate the direct effect of insulin loaded CS carbonate nanoparticle on Tyr fluorescence, free insulin sample was prepared as a reference solution. The excitation wave length was performed at 276 nm and emission spectra were recorded between 285 nm and 450 nm with the fixed slit width of 5 nm.

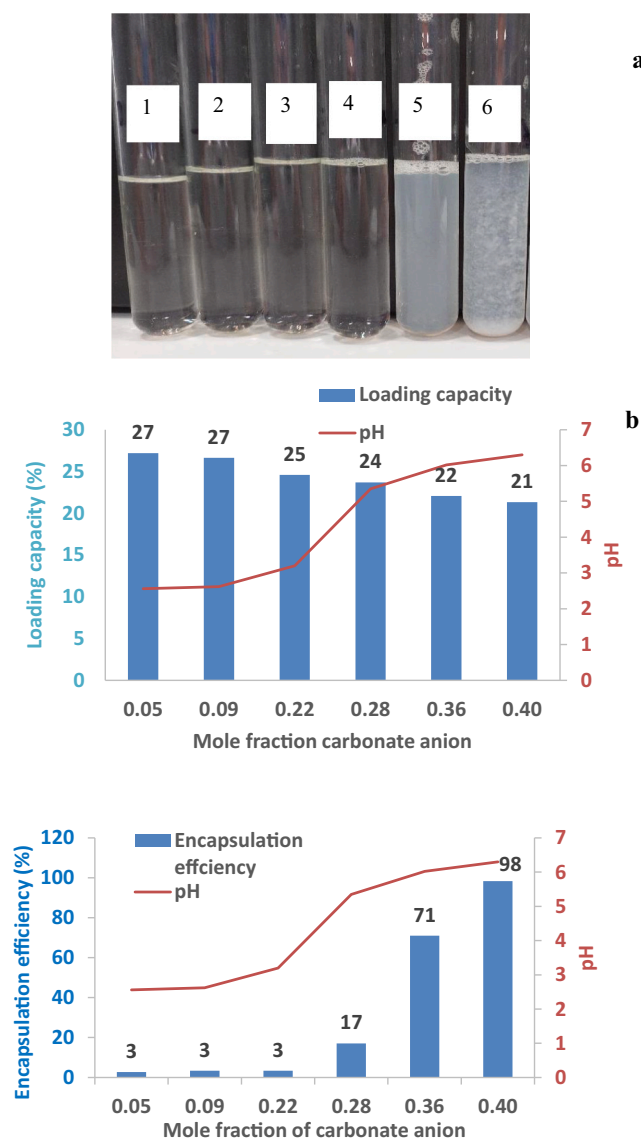


**Fig. 6.** CS carbonate loaded with insulin. (a) The prepared samples at carbonate mole fractions (1) 0, (2) 0.09, (3) 0.22, (4) 0.28, (5) 0.36 and (6) 0.4 after storage at ambient conditions for 4 h. The prepared tubes were analyzed for (b) loading capacity–pH mole fraction plot and (c) encapsulation efficiency–pH mole fraction plot.

### 3. Results and discussion

#### 3.1. Formulation and characterization of crosslinked LMW CS carbonates nanoparticles

In this study, LMW CS was used for preparation of nanoparticles since it produces a reasonable small-sized particles compared to high molecular weight candidates (Hui-Chia, 2009). CS molecular chains are extended in solution due to charge repulsion of highly protonated amino groups. The chains are expected to be accessible by the small carbonate anions, where carbonate divalent anions serve as pH neutralizer and at the same time crosslinking agent. Chain-crosslinking of CS by carbonate anions could produce compact nanoparticles as illustrated in the schematic representation in Fig. 1(a). It may also react with CS and form nano-structures that are adsorbed at the surface and reduce surface tension as discussed in surface tension measurements below. Moreover, in FTIR spectrum, the carbonyl functional group band at  $1770\text{ cm}^{-1}$  disappeared in the complex due to polymer engulfment and formation of

a highly restricted bond due to interaction between carbonate anion and amine group of CS, as shown in Fig. 1(b) (Jain & Jain, 2010). Two absorption bands appeared in the spectrum of CS crosslinked with carbonate; band at  $1640\text{ cm}^{-1}$  assigned to antisymmetric deformation N–H vibrations in  $\text{NH}_3^+$  ion and another split band at  $1112$  and  $1107\text{ cm}^{-1}$ , corresponding to antisymmetric stretching vibrations of carbonate groups, confirms the formation of ionic crosslinks between  $\text{NH}_3^+$  groups of CS and carbonate anions. Such crosslinking interactions would involve ion-ion, ion-dipole and hydrogen bonding (Gierszewska-Drużyńska & Ostrowska-Czubenko, 2011).

As a proof of this interaction, surface tension measurements were performed as shown in Fig. 2. When CS was added to water, surface tension remained constant (Al-Sou'od, 2013). However, when sodium carbonate was added to CS solution, a pronounced reduction in surface tension from  $72$  to  $40\text{ mN/m}$  occurred. Sodium carbonate induced a structural change in CS that lead to change in surface tension. The addition of crosslinking carbonate anions decreased CS nanoparticles electrostatic charges. Consequently, the repulsion force between the nanoparticles and the liquid molecules increased which enhanced the adsorption to the surface and therefore, reduced surface tension (Bhuiyan, Saidur, Amalina, Mostafizur, & Islam, 2015). Similarly, physical crosslinking of water soluble low molecular weight CS produced water-insoluble nano-structures as in the case of crosslinking of CS with pentasodium triphosphosphate, sulfate and carbonate anions (Rivas, Urbano, & Sánchez, 2018; Gierszewska & Ostrowska-Czubenko, 2016; Al-Remawi & Al-Akayleh, 2020).

The particle size changes of the dried aggregated structures were scanned in an area of  $50 \times 50\ \mu\text{m}$  using the MPP-AFM contact mode, Fig. 3.

The figure indicated the presence of relatively large aggregated dried structures ranging from  $1000$  to  $10,000\text{ nm}$  for CS, while the addition of carbonate to CS resulted in the existence of large number of nano-sized particulates ranging from  $100$  to  $300\text{ nm}$ . This could indicate the crosslinking of CS polymer chains with carbonate anions (Marques, Chagas, Fonseca, & Pereira, 2016). Furthermore, particle size and zeta potential were also measured for crosslinked CS carbonate in the aqueous state and the suitable crosslinking molar ratio was determined, as shown in Fig. 4.

Parameters that influence particle size of crosslinked CS nanoparticles would be pH, the ratio of CS to carbonate anions, condition of mixing and CS molecular weight. In this study, the parameters that influence particle size were studied simultaneously. In other studies, each parameter was investigated individually while fixing other parameters (Abdel-Hafez, Hathout, & Sammour, 2014; Asasutjarit, Sorrachaitawong, Tipchuwong, & Pouthai, 2013). In our study, the parameters are interrelated and couldn't be separated. As illustrated in Fig. 4(a), the particle size was influenced by the mole fraction of the two interacting moieties i.e. carbonate anions and glucosamine monomer cations; however, the pH of the dispersion medium was also changed with the change in mole fractions. The pH determined the density of charges on the interacting molecules and the electrostatic interaction between CS and carbonate anions. Thus, the particle size change was not dependent on change of mole fraction alone but it was a resultant of these two interacting parameters i.e. the ratio and the pH. An increase in the pH was observed with the increase of the carbonate mole fraction. This was expected, as sodium carbonate is an alkaline solution (pH about  $11.3$ ) and when it was added to acidic solution of protonated CS of pH around  $4$ , the pH increased first rapidly and then slowly. At pH  $5.5$ ,  $90\%$  of CS will be ionized since CS pKa is  $6.5$  (Athavale et al., 2022). The crosslinking of CS with carbonate ions leads to formation of smallest particle size due to CS polymer chains shrinkage. The optimal interaction based on molar fraction of carbonate and glucosamine monomer was determined to be at the lowest particle size produced. It was found to be  $0.23$  and  $0.77$  for carbonate and glucosamine monomers, respectively. Thus, approximately each molecule of carbonate divalent anion would coordinate with  $3$  molecules of glucosamine monomer monovalent cation to

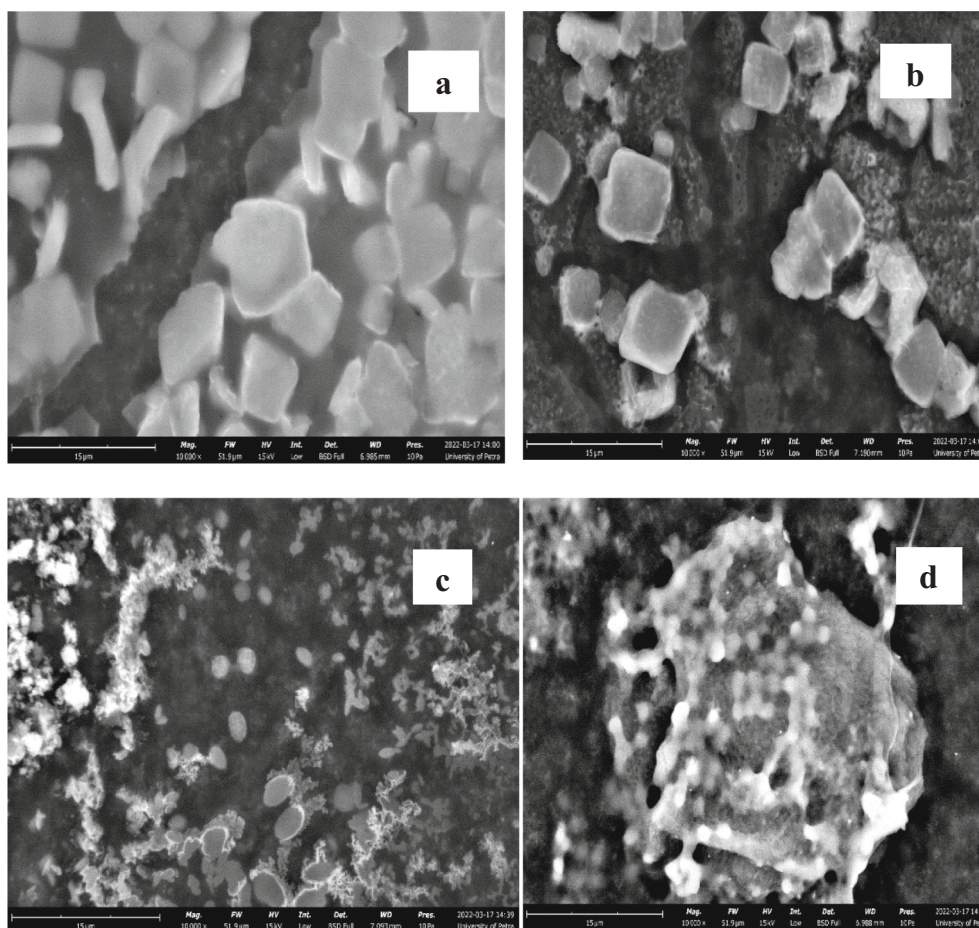


**Fig. 7.** SEM images of microstructure of insulin loaded CS carbonate preparation. Where, insulin (0.4 mg/ml) in 0.01 M HCl was subjected to carbonate anions to molar fractions (a) 0, (b) 0.28, (c) 0.36 and (d) 0.40. Images were taken at magnification 10,000 $\times$ .

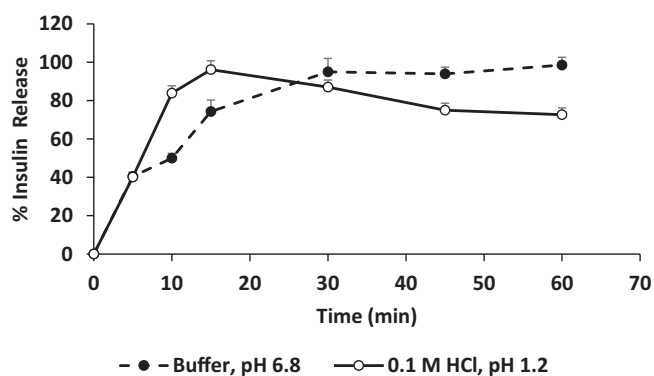


**Fig. 8.** Insulin release from insulin loaded CS carbonate (at carbonate mole fraction 0.36) in 0.1 M HCl and phosphate buffer pH 6.8.

produce the optimal smallest particle size. A steep increase of the particle size was noticed when the fraction of carbonate was further increased above 0.35, where pH became  $\geq 6.5$ . This may be due to vast neutralization of the amino functional groups i.e. more than 50% of glucosamine monomers will be neutralized, which leads to the decrease in CS solubility and aqueous dispersibility and subsequently leading to CS polymer precipitation. These results were in accordance with a previous report about particle size of CS-TPP nanoparticles, which was found to be pH sensitive (Antoniou et al., 2015). Another explanation, the reduction of particle size when pH increased up to 5.5 may be

probably caused by the reduction of repulsive interaction between positively-charged CS because CS positive charges reduced when pH increased. When pH increased from 5.5 to 7.0, loss of electrostatic interaction between CS and carbonate anions caused by neutralization of CS positive charges loosened cross-linking of nanoparticles that resulted in increase of particle sizes.

Zeta potential was also sensitive to concentration of carbonate anions and pH of the solution. The highest value [+40 mV] was noticed at pH 5.5 i.e. at carbonate mole fraction of 0.23, as shown in Fig. 4(b). This indicates that the resulted positively charged nanoparticles would have the maximum physical stability at pH 5.5. At pH below 5.5, carbonate anions act as mild counter-ions that replaces chloride counter-ions of CS glucosamine monomers. Thus, carbonate anions would not reduce the positive charge of CS nanoparticles, rather the CS folding by such crosslinking interactions leading to more shrinkage and folding CS backbone which resulted in an increase in positive charge in the CS surface charge density. Above pH 5.5, upon further addition of carbonate, glucosamine started to lose its positive charges due to pH change and thus the positive charge of CS nanoparticles started decreasing. This was evidenced by the formation of larger particle size due to instability of these systems which eventually leads to their aggregation. The use of multivalent anions to crosslink amino polymers has been described elsewhere (Al-Remawi & Al-Akayleh, 2020, Thakashnamoorthy et al., 2010).

After the addition of insulin to CS carbonate, the lowest particle size was observed at carbonate mole fraction 0.27 and pH 5.1 to 5.5 in the presence of fixed amount of insulin using different mole fractions of carbonate to CS, Fig. 5(a).

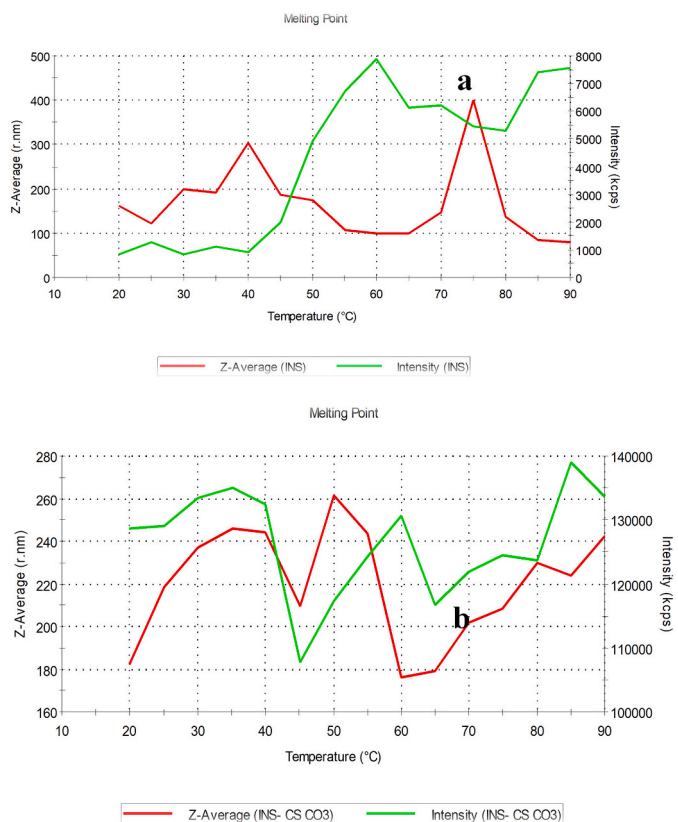


Fig. 9. Changes in Z-average and intensity of (a) insulin and (b) insulin loaded in the crosslinked CS carbonate upon heating.

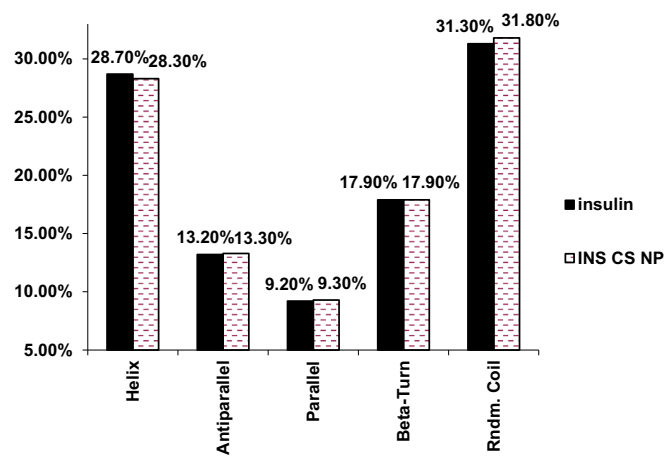


Fig. 10. The deconvolution of the CD scan in the range 190–280 nm of insulin and insulin loaded CS carbonate at 20 °C.

This result indicated the presence of insulin affected the reaction of carbonate anion to CS. It seems that more carbonate anions were required to have the lowest particle size compared to carbonate/CS without insulin. Similarly, a rapid increase in particle size was noticed when the mole fraction of carbonate was increased above 0.35, where  $pH \geq 6.5$ . Moreover, the change in zeta potential was different due to the existence of insulin. There was a reduction in surface charges of the nanoparticles prepared at different carbonate anion mole fraction, Fig. 5 (b). This could be explained by neutralization of some of CS charges with insulin. Insulin acquired negative charge above its isoelectric point (IEP) which is 5.5. pH increased almost linearly with the increase in carbonate mole fraction. Particles formed large aggregates at pH 6.5 which

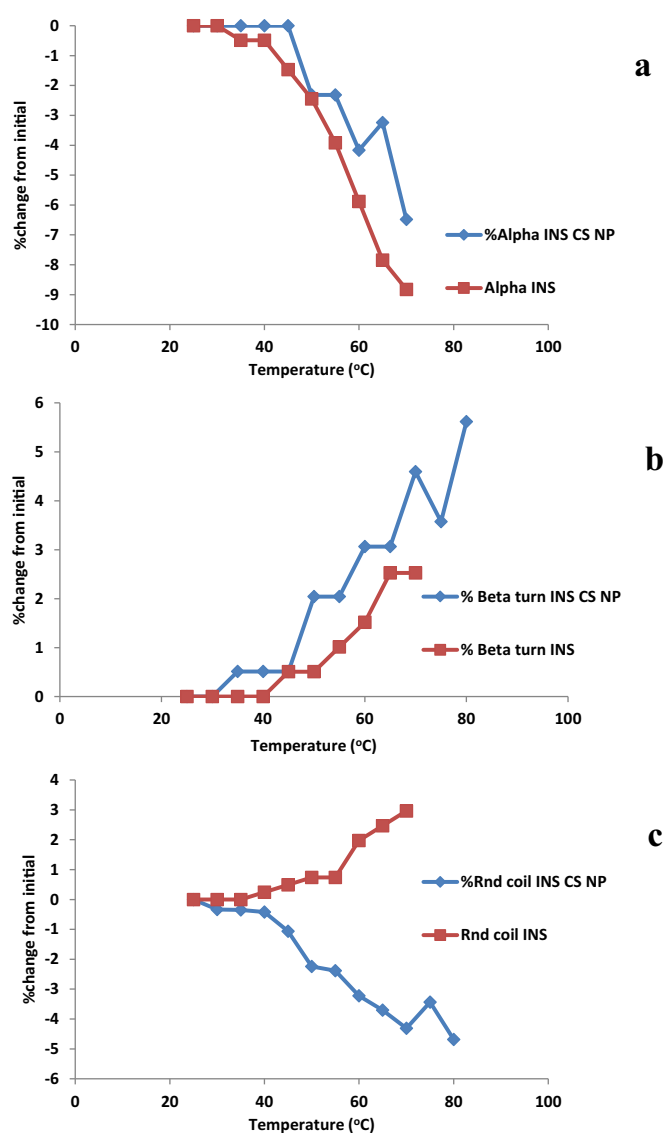


Fig. 11. Insulin secondary structure changes from their initial for insulin in water versus insulin CS carbonate in water measured at different temperatures in the range 190–280 nm: (a)  $\alpha$ -helix, (b)  $\beta$  turn and (c) random coil.

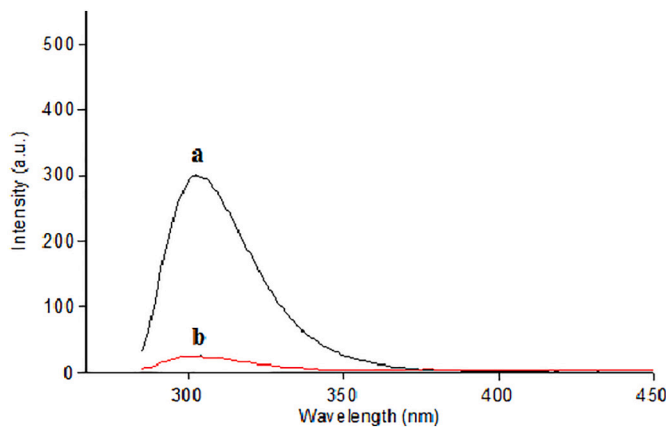


Fig. 12. Fluorescence spectra for (a) insulin and (b) insulin loaded CS carbonate nanoparticles.

coincide with the reduction in zeta potential of CS. Based on these findings, an optimum mole fraction of carbonate anion which gives a reasonable nano-size, zeta potential was selected to be 0.27.

A scheme was established to demonstrate the effect of carbonate anion addition to the formation of insulin loaded CS carbonate nanoparticles, [Scheme 1](#). At pH below 4, CS and insulin should have a positive charge with no significant interaction before the addition of carbonate anion. Upon the addition of a sufficient amount of carbonate to change the pH 5.1 to 5.5, CS started crosslinking with carbonate anion in the presence of insulin. The associated insulin started to precipitate at its IEP inside the CS carbonate nanoparticle. Further addition of carbonate anions resulted in an increase in pH above 6.5 where CS started losing its charge and precipitated and so releasing the associated insulin.

### 3.2. characterization of insulin loaded CS carbonates nanoparticles

In order to study loading capacity (LC) and encapsulation efficiency (EE) of insulin in CS carbonate nanoparticles, different mole fractions of carbonate anions to CS were added to solution containing constant insulin concentration (0.4 mg/ml). The mixture resulted in the production of insulin loaded CS carbonate nanoparticles as depicted in [Fig. 6](#). The increase in solution turbidity was noticed as the fraction of carbonate increased, as in [Fig. 6\(a\)](#). This is due to the increase in the degree of crosslinking and so precipitation produced. All the preparations showed physical stability upon storage except the preparation where carbonate was added at 0.4 mol fraction. Mole fraction 0.4 (where pH of the solution around 6.5) showed particle aggregation and precipitation.

Insulin LC in the nanoparticle system was in the range of 21–27%, [Fig. 6\(b\)](#), while the EE reached a maximum limit at carbonate anion 0.4 mol fraction (98%), [Fig. 6\(c\)](#). However, due to physical instability of formula of 0.4 mol fraction, the selected preparation for further testing was 0.36 mol fraction with EE of 71%. The high LC (>20%) and EE (>70%) are considered important properties in any nanocarrier system ([Cohen et al., 2000](#); [Liu, Yang, Jin, Xu, & Zhao, 2020](#)). These parameters directly affect the physicochemical and therapeutic effect of the system. However, results showed that the amount of insulin encapsulated was dependent on carbonate concentration and pH of the system. The entrapment efficiency increased significantly at higher carbonate mole fraction at pH in the range of 5.5 to 6.5.

SEM images of insulin loaded CS carbonate were carried out to observe the nanoparticle morphology, [Fig. 7](#). Insulin formed cubic crystalline structures in the absence of carbonate anions, [Fig. 7\(a\)](#). Similar findings were observed for insulin crystallization in acidic and alkaline solutions ([Gursky, Badger, Li, & Caspar, 1992](#); [Timofeev et al., 2010](#)).

The addition of carbonate anion in mole fraction 0.28, decreased the number of crystalline structures and at same time resulted in the production smaller sized insulin crystals, [Fig. 7\(b\)](#). Further addition of carbonate anions resulted in disappearance of insulin crystalline structures and instead nano-structures or sphere were clearly observed i.e. at molar fractions of 0.36 and 0.4, [Fig. 7\(c\)](#) & (d), respectively. Consequently, the SEM images could indicate that insulin was encapsulated in spherical smooth surface nanoparticles at carbonate to CS mole fractions higher than 0.36.

In vitro release profiles of insulin from insulin loaded CS carbonate nanoparticles (carbonate mole fraction 0.36) was performed in release media mimicking physiological pH of the stomach and buccal cavity i.e. pH values were 1.2 and 6.8, respectively at 37 °C ([Baliga, Muglikar, & Kale, 2013](#); [Liu et al., 2021](#)). Insulin showed slower release pattern behavior at pH 6.8, compared to the release in at pH 1.2, [Fig. 8](#). Thus, the nanoparticles could have less protection power to insulin in acidic condition of the stomach compared to slightly neutral pH conditions of the buccal cavity. This could indicate that such formulation could be more suitable for insulin buccal delivery.

### 3.3. Stability of insulin CS carbonates nanoparticles

In [Fig. 9\(a\)](#), traces of insulin particle size and counts rates values versus temperature were depicted. A noticeable increase in counts rates with concomitant reduction in particle size at 60 °C could be attributed to dissociation of insulin hexamers and dimers into monomers with smaller particle size and concomitant increase in particles number. Another explanation is the unfolding of insulin which, results in an increase in number of species as evidenced by tremendous increase of counts rates values at 60 °C. It is possible that the two processes were occurred consecutively, dissociation followed by unfolding. Following unfolding, inter-polymer hydrophobic interactions can lead to non-specific aggregation of the denatured polypeptide chains which occurred at 75 °C as confirmed by pronounced increase in particle size accompanied with reduction in counts rates values. This is in agreement with previous study in which the average denaturation temperature of insulin was 73.1 °C ([Mao, Bakowsky, Jintapattanakit, & Kissel, 2006](#); [Picone & Cunha, 2013](#); [Soleymani et al., 2016](#)).

When insulin was incorporated into nanoparticles, the trace was complex due to instability of the nanoparticles at higher temperatures. However, the sharp peak of insulin at 75 °C was not observed as illustrated in [Fig. 9\(b\)](#). Nanoparticles may protect insulin at high temperatures. Other studies demonstrated that CS stabilized insulin partially ([Elsayed et al., 2009](#); [Jintapattanakit et al., 2007](#)).

In order to understand the role of CS carbonate system in stabilization of insulin, circular dichroism (CD) scans were conducted at different temperatures for both insulin and CS carbonate. CD measured in far ultraviolet range was used for determination of secondary structure of proteins ([Elsayed et al., 2014](#)). CD traces of insulin and CS carbonate were displayed. In insulin and insulin loaded CS carbonate nanoparticles two minima at about 210 and 222 nm were obtained which indicated the helical structure of insulin consistent with previous reports ([Elsayed et al., 2014](#); [Sarmiento, Ferreira, Jorgensen, & Van De Weert, 2007](#)), deconvolution was carried out to illustrate the proportion of secondary structure elements for insulin and insulin-CS carbonate solutions at 20 °C, [Fig. 10](#). Both of them contain about: 28%  $\alpha$ -helix, 13% antiparallel and 9% parallel  $\beta$ -sheet, 18%  $\beta$ -turn and 32% random coil. The slight difference between the two samples could be within the software error i.e. less than 2% error. This indicates that CS carbonate didn't change the conformation of insulin. However, other studies reported higher percentage of helical structures for example the values for zinc free insulin was 57% and in another study it was 46% ([Hinds & Kim, 2002](#)). It seems that zinc content affect the proportion of  $\alpha$ -helix. Xinhua et al. related the reduction in helical element to dynamic perturbation or segmental changes in conformation ([Hua et al., 2006](#)). Exposure of insulin to air/liquid interface like in stirring or centrifugation promotes conformational changes that were detected by CD ([Hua et al., 2006](#)).

However, in this study, insulin was not exposed to any kind of stress. CD was also run at different temperatures for the two samples. The percentage changes of the secondary structure parameters at different temperatures for insulin and insulin-CS carbonate solutions were displayed in [Fig. 11](#). Both  $\alpha$ -helical and  $\beta$ -sheet structures change with temperature. It was found that  $\alpha$ -helix decreases, while  $\beta$ -sheet increases at high temperatures. Bouchard et al. also noticed a conformational change of insulin from  $\alpha$ -helical to  $\beta$ -sheet on heating to 70 °C ([Bouchard, Zurdo, Nettleton, Dobson, & Robinson, 2000](#)). Insulin CS carbonate solution was stable up to 45 °C after that the percentage of change in  $\alpha$ -helix increases with the increase in temperature. While, insulin solution in water started to change at 30 °C. The difference between free insulin and insulin-CS carbonate traces was not significant. Hua et al. attributed the reduction of  $\alpha$ -helix to static structural changes or conformational fluctuations within the helical element ([Hua et al., 2006](#)).

The major change between the two samples i.e. insulin and insulin CS carbonate solutions was on the percentage of random coil. The

percentage of random coil of insulin was not affected by temperature. In contrast, the percentage was decreased with temperature in case of insulin-CS carbonate solution. Insulin may interact with CS carbonate due to opposite charges of the two substances. CS has a positive charge and insulin bears a negative charge above its IEP point (Elsayed et al., 2014). The force of interaction increases with the increase in temperature as suggested elsewhere (Jintapattanakit et al., 2007). This interaction may decrease the unfolding of insulin and thus decrease the random coil percentage.

To prove that there was strong interaction between insulin and CS carbonate, fluorescence study was carried out. The fluorescence properties of Tyrosine [Tyr] residues can be used to follow protein-nanoparticles interaction. Insulin has four tyrosine moieties. Binding of molecules or nanoparticles to proteins often causes proteins conformation change. The emission intensity of Tyr residues is significantly affected by changing the proteins conformation (Stryer, 1968). To estimate the direct effect of CS carbonate nanoparticle on Tyr fluorescence, free insulin sample was prepared as a reference compound. The fluorescence spectra for free insulin and insulin-CS carbonate nanoparticles are shown in Fig. 12. Maximum fluorescence of insulin was recorded at 310 nm. In contrast, the spectrum of insulin-CS carbonate nanoparticles was decreased broadened and red-shifted indicating complexation between insulin and CS carbonate. Soleymani et al. observed the same phenomena when vitamin E was added to insulin (Soleymani et al., 2016).

#### 4. Conclusion

LMW CS nanoparticles were prepared based on ionic gelation. Sodium carbonate was used as a source of pH neutralizing agent and at same time it is a source of carbonate divalent. These negatively charged anion used as a crosslinking agent that interacts with the positively charged amino groups of glucosamine monomer units in CS polymer. This interaction was proved by FTIR, AFM and surface tension measurements. CS carbonate nanoparticles were prepared at different mole fractions. The optimum mole fraction of carbonate that produced the smallest size nanoparticles and highest zeta potential (median diameter 40 nm and +39 mV, respectively) was determined to be 0.23. Insulin was highly associated to nanoparticles with an association efficiency about 98%. After the addition of insulin, the smallest particle size for insulin loaded CS carbonate nanoparticles were obtained at carbonate mole fraction 0.27 and the optimal pH for interaction was 5.1 to 5.5. Insulin was not released upon dilution of insulin loaded CS carbonate nanoparticles with water. It is also noteworthy that these robust nanoparticles protected insulin at high temperatures and so could preserve its biological activity. The findings from this investigation showed the potential use of CS carbonate as an insulin stabilizer and at the same time as an insulin nanocarrier system. The in vivo work will be carried out in future to prove their potential role in facilitating insulin buccal delivery.

#### CRedit authorship contribution statement

**Mayyas Al-Remawi:** Conceptualization, Supervision, Writing – original draft. **Nisrein Jaber:** Methodology, Writing – review & editing. **Amani Elsayed:** Writing – original draft. **Diya Alsafadi:** Methodology, Investigation. **Khalid Abu Salah:** Visualization.

#### Declaration of competing interest

The authors declare that they have no known competing financial interests or personal relationships that could have appeared to influence the work reported in this paper.

#### Acknowledgement

Authors would like to thank Deanship of Scientific Research at

University of Petra for funding this project.

#### References

- Abdel-Hafez, S. M., Hathout, R. M., & Sammou, O. A. (2014). Towards better modeling of chitosan nanoparticles production: Screening different factors and comparing two experimental designs. *International Journal of Biological Macromolecules*, 64, 334–340.
- Al-Remawi, M. M. (2012). Properties of chitosan nanoparticles formed using sulfate anions as crosslinking bridges. *American Journal of Applied Sciences*, 9(7), 1091.
- Al-Remawi, M., Elsayed, A., Maghrabi, I., Hamaidi, M., & Jaber, N. (2017). Chitosan/lecithin liposomal nanovesicles as an oral insulin delivery system. *Pharmaceutical Development and Technology*, 22(3), 390–398.
- Al-Sou'od, K. (2013). Surface activity of some low molecular weight chitosan derivatives. *Jordan Journal of Chemistry (JJC)*, 8(1), 1–17.
- Antoniu, J., Liu, F., Majeed, H., Qi, J., Yokoyama, W., & Zhong, F. (2015). Physicochemical and morphological properties of size-controlled chitosan-tripolyphosphate nanoparticles. *Colloids and Surfaces A: Physicochemical and Engineering Aspects*, 465, 137–146.
- Asasutjarit, R., Sorrachaitawatwong, C., Tipchuwong, N., & Pouthai, S. (2013). Effect of formulation compositions on particle size and zeta potential of diclofenac sodium-loaded chitosan nanoparticles. *International Journal of Pharmacological and Pharmaceutical Sciences*, 7(9), 568–570.
- Athavale, R., Sapre, N., Rale, V., Tongaonkar, S., Manna, G., Kulkarni, A., & Shirolkar, M. M. (2022). Tuning the surface charge properties of chitosan nanoparticles. *Materials Letters*, 308, Article 131114.
- Badwan, A., Remawi, M., Qinna, N., Elsayed, A., Arafat, T., Melhim, M., & Idkaidek, N. M. (2009). Enhancement of oral bioavailability of insulin in humans.
- Bagheri, M., Younesi, H., Hajati, S., & Borghei, S. M. (2015). Application of chitosan-citric acid nanoparticles for removal of chromium (VI). *International Journal of Biological Macromolecules*, 80, 431–444.
- Baliga, S., Muglikar, S., & Kale, R. (2013). Salivary pH: A diagnostic biomarker. *Journal of Indian Society of Periodontology*, 17(4), 461.
- Bhuiyan, M. H. U., Saidur, R., Amalina, M. A., Mostafizur, R. M., & Islam, A. K. M. S. (2015). Effect of nanoparticles concentration and their sizes on surface tension of nanofluids. *Procedia Engineering*, 105, 431–437.
- Bouchard, M., Zurdo, J., Nettleton, E. J., Dobson, C. M., & Robinson, C. V. (2000). Formation of insulin amyloid fibrils followed by FTIR simultaneously with CD and electron microscopy. *Protein Science*, 9(10), 1960–1967.
- Cabaleiro-Lago, O. S., & Lins, S. (2012). The effect of nanoparticles on amyloid aggregation depends on the protein stability and intrinsic aggregation rate. *Langmuir*, 28(3), 1852–1857.
- Chen, M. C., Mi, F. L., Liao, Z. X., Hsiao, C. W., Sonaje, K., Chung, M. F., Sung, H. W., ... (2013). Recent advances in chitosan-based nanoparticles for oral delivery of macromolecules. *Advanced Drug Delivery Reviews*, 65(6), 865–879.
- Cohen, H., Levy, R. J., Gao, J., Fishbein, I., Kousaev, V., Sosnowski, S., Golomb, G., ... (2000). Sustained delivery and expression of DNA encapsulated in polymeric nanoparticles. *Gene Therapy*, 7(22), 1896–1905.
- Das, A., Chakrabarti, A., & Das, P. K. (2015). Suppression of protein aggregation by gold nanoparticles: A new way to store and transport proteins. *RSC Advances*, 5, 38558–38570.
- Diop, M., Auberval, N., Viciglio, A., Langlois, A., Bietiger, W., Mura, C., Sigrist, S., ... (2015). Design, characterisation, and bioefficacy of insulin-chitosan nanoparticles after stabilisation by freeze-drying or cross-linking. *International Journal of Pharmaceutics*, 491(1–2), 402–408.
- Du, Y., Luo, X. L., Xu, J. J., & Chen, H. Y. (2007). A simple method to fabricate a chitosan-gold nanoparticles film and its application in glucose biosensor. *Bioelectrochemistry*, 70(2), 342–347.
- Elsayed, A., Al-Remawi, M., Qinna, N., Farouk, A., & Badwan, A. (2009). Formulation and characterization of an oily-based system for oral delivery of insulin. *European Journal of Pharmaceutics and Biopharmaceutics*, 73(2), 269–279.
- Elsayed, A., Al-Remawi, M., Maghrabi, I., Hamaidi, M., & Jaber, N. (2014). Development of insulin loaded mesoporous silica injectable particles layered by chitosan as a controlled release delivery system. *International Journal of Pharmaceutics*, 461(1–2), 448–458.
- Elsayed, A., Al-Remawi, M., Qinna, N., Farouk, A., Al-Sou'od, K. A., & Badwan, A. A. (2011). Chitosan-sodium lauryl sulfate nanoparticles as a carrier system for the in vivo delivery of oral insulin. *AAPS PharmSciTech*, 12(3), 958–964.
- Gierszewska, M., & Ostrowska-Czubenko, J. (2016). Equilibrium swelling study of crosslinked chitosan membranes in water, buffer and salt solutions. *Progress on Chemistry and Application of Chitin and its Derivatives*, 21, 55–62.
- Gierszewska-Drużyńska, M., & Ostrowska-Czubenko, J. (2011). Influence of crosslinking process conditions on molecular and supermolecular structure of chitosan hydrogel membrane. *Progress on Chemistry and Application of Chitin and its Derivatives*, 16, 15–22.
- Grenha, A. (2012). Chitosan nanoparticles: A survey of preparation methods. *Journal of Drug Targeting*, 20(4), 291–300.
- Gursky, O., Badger, J., Li, Y., & Caspar, D. L. (1992). Conformational changes in cubic insulin crystals in the pH range 7–11. *Biophysical Journal*, 63(5), 1210–1220.
- Hinds, K. D., & Kim, S. W. (2002). Effects of PEG conjugation on insulin properties. *Advanced Drug Delivery Reviews*, 54(4), 505–530.

- Hua, Q. X., Nakagawa, S., Hu, S. Q., Jia, W., Wang, S., & Weiss, M. A. (2006). Toward the active conformation of insulin: Stereospecific modulation of a structural switch in the B chain. *Journal of Biological Chemistry*, 281(34), 24900–24909.
- Hui-Chia, Y. (2009). I min-Hsiung H.: The effect of the molecular weight of chitosan nanoparticles and its application on drug delivery. *Microchemical Journal*, 92(1), 87–91.
- Jain, N. K., & Jain, S. K. (2010). Development and in vitro characterization of galactosylated low molecular weight chitosan nanoparticles bearing doxorubicin. *AAPS PharmSciTech*, 11(2), 686–697.
- Jarrar, Y. B., Al-Essa, L., Kilani, A., Hasan, M., & Al-Qerem, W. (2018). Alterations in the gene expression of drug and arachidonic acid-metabolizing Cyp450 in the livers of controlled and uncontrolled insulin-dependent diabetic mice. *Diabetes, Metabolic Syndrome and Obesity: Targets and Therapy*, 11, 483.
- Jayamani, J., & Shanmugam, G. (2016). Gelatin as a potential inhibitor of insulin amyloid fibril formation. *ChemistrySelect*, 1, 4463–4471.
- Jintapattanakit, A., Junyaprasert, V. B., Mao, S., Sitterberg, J., Bakowsky, U., & Kissel, T. (2007). Peroral delivery of insulin using chitosan derivatives: A comparative study of polyelectrolyte nanocomplexes and nanoparticles. *International Journal of Pharmaceutics*, 342(1–2), 240–249.
- Kar, N. R., & Pati, K. C. (2019). Effect of cross linking on evaluation of chitosan coated pellets of glipizide. *Journal of Drug Delivery and Therapeutics*, 9(4-A), 237–245.
- Lari, A. S., Zahedi, P., Ghourchian, H., & Khatibi, A. (2021). Microfluidic-based synthesized carboxymethyl chitosan nanoparticles containing metformin for diabetes therapy: In vitro and in vivo assessments. *Carbohydrate Polymers*, 261, Article 117889.
- Lee, C., Choi, J. S., Kim, I., Oh, K. T., Lee, E. S., Park, E. S., Youn, Y. S., ... (2013). Long-acting inhalable chitosan-coated poly (lactic-co-glycolic acid) nanoparticles containing hydrophobically modified exendin-4 for treating type 2 diabetes. *International Journal of Nanomedicine*, 8, 2975.
- Lin, Y. H., Chung, C. K., Chen, C. T., Liang, H. F., Chen, S. C., & Sung, H. W. (2005). Preparation of nanoparticles composed of chitosan/poly- $\gamma$ -glutamic acid and evaluation of their permeability through Caco-2 cells. *Biomacromolecules*, 6(2), 1104–1112.
- Liu, R., Wu, Q., Huang, X., Zhao, X., Chen, X., Chen, Y., Song, Y., ... (2021). Synthesis of nanomedicine hydrogel microcapsules by droplet microfluidic process and their pH and temperature dependent release. *RSC Advances*, 11(60), 37814–37823.
- Liu, Y., Yang, G., Jin, S., Xu, L., & Zhao, C. X. (2020). Development of high-drug-loading nanoparticles. *ChemPlusChem*, 85(9), 2143–2157.
- Lu, B., Lv, X., & Le, Y. (2019). Chitosan-modified PLGA nanoparticles for control-released drug delivery. *Polymers*, 11(2), 304.
- Ma, Z., & Lim, L. Y. (2003). Uptake of chitosan and associated insulin in Caco-2 cell monolayers: A comparison between chitosan molecules and chitosan nanoparticles. *Pharmaceutical Research*, 20(11), 1812–1819.
- Maggio, E. T. (2012). Polysorbates, peroxides, protein aggregation, and immunogenicity a growing concern. *Journal of Excipients and Food Chemicals*, 3(2), 45–53.
- Mao, S., Bakowsky, U. D. O., Jintapattanakit, A., & Kissel, T. (2006). Self-assembled polyelectrolyte nanocomplexes between chitosan derivatives and insulin. *Journal of Pharmaceutical Sciences*, 95(5), 1035–1048.
- Marques, J. S., Chagas, J. A. O. D., Fonseca, J. L. C., & Pereira, M. R. (2016). Comparing homogeneous and heterogeneous routes for ionic crosslinking of chitosan membranes. *Reactive and Functional Polymers*, 103, 156–161.
- Obaidat, R., Al-Jbour, N., Al-Sou'd, K., Sweidan, K., Al-Remawi, M., & Badwan, A. (2010). Some physico-chemical properties of low molecular weight chitosans and their relationship to conformation in aqueous solution. *Journal of Solution Chemistry*, 39(4), 575–588.
- Pelegri-O'Day, E., Bhattacharya, A., Theopold, N., Ko, J., & Maynard, H. (2020). Synthesis of zwitterionic and trehalose polymers with variable degradation rates and stabilization of insulin. *Biomacromolecules*, 21(6), 2147–2154.
- Piccinini, A., Lourenço, E. C., Ascenso, O. S., Ventura, M. R., Amenitsch, H., Moretti, P., Mariani, P., Ortore, M. G., & Spinozzi, F. (2022). SAXS reveals the stabilization effects of modified sugars on model proteins. *Life*, 12(1), 123–148.
- Picone, C. S. F., & Cunha, R. L. (2013). Chitosan–gellan electrostatic complexes: Influence of preparation conditions and surfactant presence. *Carbohydrate Polymers*, 94(1), 695–703.
- Qandil, A. M., Obaidat, A. A., Ali, M. A. M., Al-Taani, B. M., Tashatoush, B. M., Al-Jbour, N. D., Al-Remawi, M., Al-Sou'od, K., & Badwan, A. A. (2009). Investigation of the interactions in complexes of low molecular weight chitosan with ibuprofen. *Journal of Solution Chemistry*, 38(6), 695–712.
- Rasmussen, T., Tantipolphan, R., van de Weert, M., & Jiskoot, W. (2010). The molecular chaperone  $\alpha$ -crystallin as an excipient in an insulin formulation. *Pharmaceutical Research*, 27, 1337–1347.
- Raut, I. D., Doijad, R. C., Mohite, S. K., & Manjappa, A. S. (2018). Preparation and characterization of solid lipid nanoparticles loaded with cisplatin. *Journal of Drug Delivery and Therapeutics*, 8(6), 125–131.
- Rivas, B. L., Urbano, B. F., & Sánchez, J. (2018). Water-soluble and insoluble polymers, nanoparticles, nanocomposites and hybrids with ability to remove hazardous inorganic pollutants in water. *Frontiers in Chemistry*, 6, 320.
- Rull, J. A., Aguilar-Salinas, C. A., Rojas, R., Rios-Torres, J. M., Gómez-Pérez, F. J., & Olaiz, G. (2005). Epidemiology of type 2 diabetes in Mexico. *Archives of Medical Research*, 36(3), 188–196.
- Sarmento, B., Ferreira, D. C., Jorgensen, L., & Van De Weert, M. (2007). Probing insulin's secondary structure after entrapment into alginate/chitosan nanoparticles. *European Journal of Pharmaceutics and Biopharmaceutics*, 65(1), 10–17.
- Sharma, D., Arora, S., Banerjee, A., & Singh, J. (2021). Improved insulin sensitivity in obese-diabetic mice via chitosan nanomicelles mediated silencing of pro-inflammatory adipocytokines. *Nanomedicine: Nanotechnology, Biology and Medicine*, 33, Article 102357.
- Soleymani, H., Saboury, A. A., Moosavi-Movahedi, A. A., Rahmani, F., Maleki, J., Yousefinejad, S., & Maghami, P. (2016). Vitamin E induces regular structure and stability of human insulin, more intense than vitamin D3. *International Journal of Biological Macromolecules*, 93, 868–878.
- Stryer, L. (1968). Fluorescence spectroscopy of proteins: Fluorescent probes provide insight into the structure, interactions, and dynamics of proteins. *Science*, 162(3853), 526–533.
- Thakashinamoorty et al., 2010. C Thakashinamoorty S Vijayaraghavan K Kaliaperumal G Kanchivakkam Ramaswamy P Nataraj A Somasundaran N. Kaliyan Process for the preparation of carbonate salts of cross-linked amine polymers. WIPO (PCT) patent number (WO2010041274) date of publication: 15.04.2010.
- Timofeev, V. I., Chuprov-Netochin, R. N., Samigina, V. R., Bezuglov, V. V., Miroshnikov, K. A., & Kuranova, I. P. (2010). X-ray investigation of gene-engineered human insulin crystallized from a solution containing polysialic acid. *Acta Crystallographica Section F: Structural Biology and Crystallization Communications*, 66(3), 259–263.